SECOND EUROPEAN CONFERENCE ON EARTHQUAKE ENGINEERING
AND SEISMOLOGY, ISTANBUL AUG. 25-29, 2014

DYNAMIC RESPONSE OF SEABED-RUBBLE MOUND BREAKWATER SYSTEM UNDER SEISMIC WAVES

M. B. Can ÜLKER[1]

ABSTRACT

In the design of coastal structures, evaluation of dynamic response and stability of foundation materials is important. One of the major concerns related to these structures is the response of the underlying seabed under major wave action caused by ocean waves and seismic activity. Progressive or breaking surface waves induce cyclic or transient pressures on the underlying seabed soil. Additionally, seismic waves apply shear stresses to soil layers which should also be investigated particularly in earthquake prone regions. In this study, a rubble-mound breakwater (RMB) structure in the east coast of Japan lying above a seabed layer is considered. The objective is to evaluate the preliminary seismic wave-induced dynamic response of the system while eliminating hydrodynamic wave effects but maintaining hydrostatic pressures on the seabed and the rubble surface. The seabed-RMB system is modeled using finite elements and the dynamic response is assumed to be governed by the equations of coupled flow (of pore water) and deformation (of soil skeleton) of poro-elasticity. RMB is also modeled through this formulation assuming a relatively lower hydraulic conductivity including a core layer. While it is possible to derive three formulations of *fully dynamic* (FD), *partially dynamic* (PD) and *quasi-static* (QS) with respect to the inclusion of inertial terms associated with pore water and the solid part, considering the range of frequency of seismic waves, only the PD formulation is used in the analyses neglecting the inertia of pore water in the dynamic response. That is, although the FD formulation is the most complete one in terms of inertial terms, PD idealization where only the inertia associated with soil skeleton is considered, is sufficient to model the dynamic response of the system. It is found that even though pore pressures increase along the edges of the core, displacements are decreased and the stresses are concentrated highly in the RMB which tends to increase the stability during seismic shearing.

INTRODUCTION

Wave-induced dynamic response of coastal and offshore structures has been investigated over the past few decades. Majority of these works focused on the response and instability of these structures and their foundations under a severe wave storm potentially leading to catastrophic failure of the entire system. Instability due to liquefaction in seabed has been one of the significant causes of failure of such structures (Zen et al. 1986; Maeno and Nago, 1988; de Groot et al. 2006). In order to understand the mechanism behind and determine the conditions resulting in these failures, analytical, numerical and experimental studies have been conducted. As far as analytical and numerical approaches are concerned, response of porous seabed and rubble is generally formulated in the framework of the theory proposed by Biot (1941) who subsequently extended the formulation to include dynamic terms (Biot, 1955, 1962). There have been few studies thus far carried out using various approaches such as Mase et al. (1994), Jeng et al. (2001) and Ulker et al. (2010) who used finite element (FE) method to

[1] PhD., Assoc. Prof., İstanbul Technical University, İstanbul TURKEY, mbulker@itu.edu.tr

analyze the response of seabed and rubble mound around a caisson breakwater under pulsating loads. Ulker et al. (2012) modeled the dynamic response and instability of the same system under breaking waves. In these analyses the breakwater model was assumed to be a porous medium as well. As for RMB, dissipation of the incoming wave energy is due to wave breaking on its slopes and through absorption rather than reflection. Earlier studies on such structures were largely empirical in nature and ignored the effects of internal wave-induced flow and stresses. Later, these were considered with varying degrees of completeness (Oumeraci and Partensky, 1990; Losada et al., 2008). Barends et al. (1983) suggests that liquefaction in seabed caused by wave action may trigger a collapse from the toe of the breakwater and a slip down of armor units. Response of underlying seabed has later been considered (Mase et al. 1994). van Gent (1995) used physical model tests to verify their numerical model which calculates the wave motion and its related effect on a berm breakwater. Palmer and Christian (1998) studied some design aspects of a RMB. If not liquefaction, stability of such structures may be endangered by the accumulation of irreversible strains due to cyclic shearing. Additionally, large impact forces caused by wave slamming against inclined walls of these breakwaters may cause further deformation of the seabed underneath. Hur et al. (2008) studied nonlinear dynamic interaction between waves, seabed and a submerged breakwater through numerical simulation. Referring to only a few studies carried out to model the response of a breakwater-seabed system under seismic activity, Memos et al. (2000) studied the stability of such a system utilizing numerical means. They have verified their numerical results with a set of shaking table tests for two breakwater foundations. Failures of RMBs due to seismic loading have also been reported in the past, (Memos and Protonotarios, 1992).

In this study, dynamic response of an existing RMB-seabed system is presented in terms of effective and shear stress as well as pore pressure distributions underneath the breakwater assuming plane strain stress state (Fig. 1). Seismic waves are considered to be harmonic in terms of the components of an equivalent irregular seismic record. Effect of wave frequency and the presence of a core on the dynamic response of the system are investigated through a set of parametric studies.

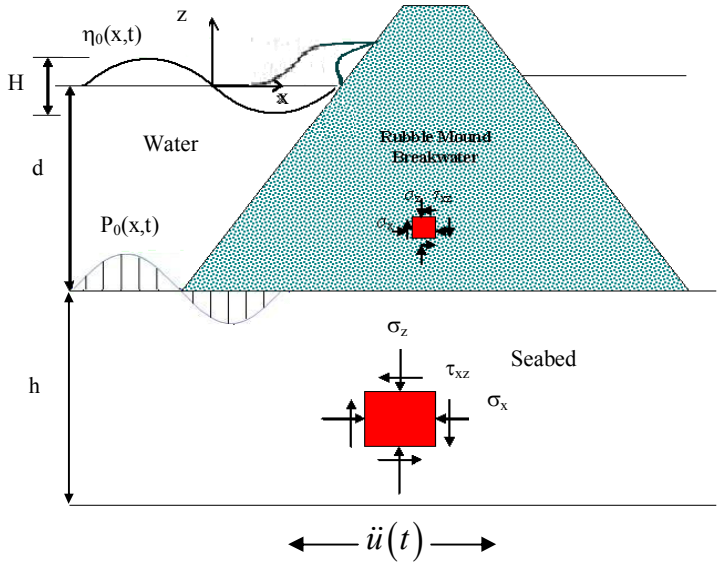

Figure 1. Rubble mound breakwater – seabed interaction

MATHEMATICAL FORMULATION

Considering the saturated (or nearly saturated) porous medium being composed of solid grains and of a viscous fluid (generally water), it can be viewed as a two phase material with both phases behaving collectively as a continuous medium. In developing a general mathematical formulation governing the response of this two phase continuum, the following assumptions are made:

1. The water and the gas phases within the porous medium are considered as a single compressible fluid.
2. The effects of gas diffusing through water and movement of water vapor are ignored.

One can think of a number of problems in geotechnical earthquake engineering where the soil is modeled under the same assumptions (Fig. 2). As for the mathematical formulation of seabed under waves, first and foremost the effective stress relation should be defined;

$$\sigma_{ij}' = \sigma_{ij} - \delta_{ij} p \tag{1}$$

followed by the stress-strain relation as,

$$\sigma_{ij}' = D_{ijkl}(\varepsilon_{kl} - \varepsilon_{kl}^{0}) \tag{2}$$

where D_{ijkl} is the constitutive material matrix and ε_{kl}^{0} is initial strain. For plane strain isotropic elasticity, the above equation in terms of Lame's parameters, λ and G becomes:

$$\sigma_{ij}' = \lambda \varepsilon_{kk} \delta_{ij} + 2G\varepsilon_{ij} \tag{3}$$

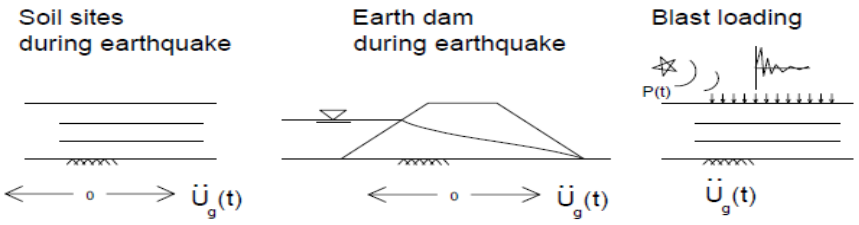

Figure 2. Various problems in geotechnical earthquake engineering

For a unit total volume, overall equilibrium of the system can be written as:

$$\sigma_{ij,j} + \rho g = \rho_w \ddot{\bar{w}} + \rho \ddot{u} \tag{4}$$

where σ_{ij} is total stress; ρ and ρ_w are the densities of the mixture and water; $\ddot{u}$ is the acceleration of the soil skeleton, $\bar{w}$ is defined as the average displacement of water relative to the soil solids and that $\ddot{\bar{w}} = d^2\bar{w}/dt^2$ is the average acceleration of pore water relative to that of soil solids which is equal to $n\ddot{w}$ with porosity n. Subscript '$,j$' indicates the derivative with respect to spatial variation. Using the Darcy's Law with a hydraulic conductivity coefficient, k_i, the equation of pore water equilibrium can be written as:

$$-p_{,i} + \rho_f g_i - \frac{\dot{\bar{w}}_i}{k_i}\rho_f g_i - \rho_f \ddot{u}_i - \frac{\rho_f}{n}\ddot{\bar{w}}_i = 0 \tag{5}$$

The mass balance equation completes the governing system,

$$\dot{\varepsilon}_{ii} + \dot{\bar{w}}_{i,i} = -\frac{n}{K_f}\dot{p} \tag{6}$$

where K_f is the bulk modulus of pore water. For only slight unsaturation (i.e. S still close to 1), pore water can be treated as a single phase and the effect can be captured by simply modifying the water compressibility (Rahman et al., 1994) as,

$$\bar{\beta} = \frac{1}{K_f} = \frac{1}{K_w} + \frac{1-S}{p_0} \tag{7}$$

with K_w as the bulk modulus of water and p_0, the reference atmospheric pressure.

FINITE ELEMENT ANALYSIS

The equations presented previously are grouped together forming a coupled system in terms of displacement and pore pressure (u - p) for the PD formulation eliminating the acceleration terms associated with the relative pore water motion ($\ddot{\bar{w}}_i$);

$$\sigma_{ij} + \rho g - \rho \ddot{u}_i = 0 \tag{8a}$$

$$\dot{u}_{i,i} + \left[\frac{k_i}{\rho_f g} \left(-p_{,i} + \rho_f g - \rho_f \ddot{u}_i \right) \right]_{,i} + \frac{n}{K_f} \dot{p} = 0 \tag{8b}$$

In the second term of (8b), effect of inertial force of the solid part to equilibrium of pore water is neglected in some studies, but is considered here in both left hand side and the right hand side force vector as presented below. The weak form of the equations (8) is,

$$\int_\Omega \delta u^T \nabla \sigma d\Omega + \int_\Omega \delta u^T \rho g d\Omega - \int_\Omega \delta u^T \rho \ddot{u} d\Omega = 0 \tag{9a}$$

$$\int_\Omega \delta p^T \nabla \dot{u} d\Omega + \int_\Omega \delta p^T \nabla^T \left[\frac{k}{\rho_f g} \left(-\nabla p + \rho_f g - \rho_f \ddot{u} \right) \right] d\Omega + \int_\Omega \delta p^T \frac{n}{K_f} \dot{p} d\Omega = 0 \tag{9b}$$

By doing integration by parts and substituting the constitutive relation for effective stress, (1), to (9a), we get,

$$\int_\Omega (\nabla \delta u)^T \left(\underset{\sim}{D} \nabla u \right) d\Omega - \int_\Omega (\nabla \delta u)^T (p) d\Omega + \int_\Omega \delta u^T \rho \ddot{u} d\Omega = \int_\Gamma \delta u^T \sigma d\Gamma + \int_\Omega \delta u^T \rho g d\Omega \tag{10a}$$

$$\begin{aligned} &\int_\Omega \delta p^T \nabla \dot{u} d\Omega + \int_\Omega (\nabla \delta p)^T \frac{[k]}{\rho_f g} \left(\nabla p + \rho_f \ddot{u} \right) d\Omega + \int_\Omega \delta p^T \frac{n}{K_f} \dot{p} d\Omega \\ &= \int_\Gamma \delta p^T \frac{[k]}{\rho_f g} \nabla p d\Gamma + \int_\Omega (\nabla \delta p)^T \frac{[k]}{\rho_f g} \left(\rho_f g \right) d\Omega \end{aligned} \tag{10b}$$

Approximating the field variables u and p in the regular FE sense yields,

$$\begin{aligned} &\left(\int_\Omega (\nabla N_u)^T [E] (\nabla N_u) d\Omega \right) U - \left(\int_\Omega (\nabla N_u)^T \{m\} N_p d\Omega \right) P + \left(\int_\Omega N_u{}^T \rho N_u d\Omega \right) \ddot{U} \\ &= \int_\Gamma N_u{}^T \sigma d\Gamma + \int_\Omega N_u{}^T \rho g d\Omega \end{aligned} \tag{11a}$$

$$\left(\int_{\Omega} Np^T \{m\}^T \nabla N u d\Omega\right)\dot{U} + \left(\int_{\Omega} (\nabla Np)^T \frac{[k]}{\rho_f g} \nabla Np d\Omega\right) P + \left(\int_{\Omega} (\nabla Np)^T \frac{[k]}{g} Nud\Omega\right)\ddot{U} + \left(\int_{\Omega} Np^T \frac{n}{K_f} Np d\Omega\right)\dot{P} = \int_{\Gamma} (Np)^T \frac{[k]}{\rho_f g}(\nabla p) d\Gamma + \int_{\Omega} (Np)^T \frac{[k]}{\rho_f g}(\rho_f g) d\Omega \tag{11b}$$

These equations can also be written in a matrix form as,

$$\begin{aligned} &\mathbf{K_s}\{U\} - \mathbf{C}\{P\} + \mathbf{M_s}\{\ddot{U}\} = \{F_s\} \\ &\mathbf{C}^T\{\dot{U}\} + \mathbf{K_f}\{P\} + \mathbf{M_{sf}}\{\ddot{U}\} + \mathbf{C_f}\{\dot{P}\} = \{F_f\} \end{aligned} \tag{12}$$

or in combined matrix form as,

$$\begin{bmatrix} \mathbf{M_s} & 0 \\ \mathbf{M_{sf}} & 0 \end{bmatrix}\begin{Bmatrix} \ddot{\boldsymbol{U}} \\ \ddot{\boldsymbol{P}} \end{Bmatrix} + \begin{bmatrix} 0 & 0 \\ \mathbf{C^T} & \mathbf{C_f} \end{bmatrix}\begin{Bmatrix} \dot{\boldsymbol{U}} \\ \dot{\boldsymbol{P}} \end{Bmatrix} + \begin{bmatrix} \mathbf{K_s} & \mathbf{-C} \\ 0 & \mathbf{K_f} \end{bmatrix}\begin{Bmatrix} \boldsymbol{U} \\ \boldsymbol{P} \end{Bmatrix} = \begin{Bmatrix} \boldsymbol{F_s} \\ \boldsymbol{F_f} \end{Bmatrix} \tag{13}$$

The stiffness matrices are; $\mathbf{K_s} = \int_{\Omega} [B_u]^T \underset{\sim}{D} [B_u] d\Omega$, $\mathbf{K_f} = \int_{\Omega} [B_p]^T \frac{[k]}{\rho_f g} [B_p] d\Omega$, damping matrices are $\mathbf{C} = \int_{\Omega} [B_u]^T \{m\} [N_p] d\Omega$ which is also the coupling matrix and $\mathbf{C_f} = \int_{\Omega} [N_p]^T \frac{n}{K_f} [N_p] d\Omega$ and the mass matrices are $\mathbf{M_s} = \int_{\Omega} [N_u]^T \rho [N_u] d\Omega$, $\mathbf{M_{sf}} = \int_{\Omega} [B_p]^T \frac{[k]}{g} [N_u] d\Omega$. The force vectors are also evaluated as, $F_f = \int_{\Gamma} [N_p]^T \left(\frac{[k]}{\rho_f g}\right)(n^T p) d\Gamma + \int_{\Omega} [N_p]^T \frac{[k]}{\rho_f g}(\rho_f g) d\Omega$, $F_s = \int_{\Gamma} [N_u]^T \{\sigma\} d\Gamma + \int_{\Omega} N_u{}^T \rho g d\Omega$.

Eight node quadrilaterals, (Q8), and their shape functions are used for quadratic approximation of the displacement degree of freedom (DOF) and four node (Q4) is used for pore pressure DOF. Gauss quadrature numerical integration method with reduced 2x2 integration rule is chosen for the numerical integration of both fields.

The breakwater model is obtained considering an existing structure in the coastal region of Japan (Mase et al., 1994). FE model can be seen in Fig. 3. The boundary conditions satisfying the linear system of equations defined are specified as;

$$\begin{aligned} &n_x(\sigma_{xx} - p) + n_z \sigma_{xz} = -n_x p \\ &n_x \sigma_{zx} + n_z(\sigma_{zz} - p) = -n_z p \end{aligned} \quad \text{on} \quad \Gamma_1 \cup \Gamma_2 \cup \Gamma_3 \cup \Gamma_4 \cup \Gamma_6 \tag{14}$$

where n_x and n_z are the direction cosines and

$$p = \rho_w g d \tag{15}$$

along the boundaries Γ_1 through Γ_4 as hydrostatic pressure. Although using absorbing boundaries along the lateral surfaces is the best way to model the problem (which helps eliminate any reflecting waves from the artificial boundaries), with no access to such boundary condition (as of now which is currently being implemented), it is assumed that the soil vibrates in the horizontal direction in the

same frequency as the incoming wave and that, all the wave effect disappears in the far distance with no additional hydrodynamic waves leading to $u_z = p = 0$ on Γ_5. This way, some effect of wave reflection is tried to be surpassed. At the bottom impermeable boundary, Γ_6, $u_z = \frac{\partial p}{\partial \mathbf{n}} = 0$. However, seismic wave is now applied in terms of harmonic displacement along Γ_6 as $u(t) = -cos(\omega t)/\omega^2$ with frequency, ω. As for Γ_7, to handle the flow boundary condition, bottom shaking of a layer of seabed in the free field (with no structure) is considered and corresponding DOF results are applied as time histories along the left lateral surface as was previously done by Ulker et al. (2010) in the case of surface waves.

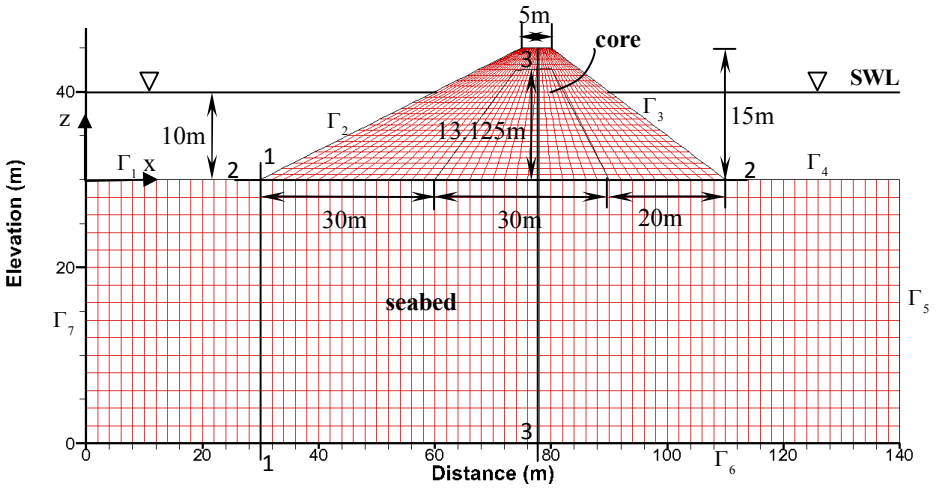

Figure 3. FE model of rubble mound breakwater with core as used by Mase et al. (1994)

INITIAL DYNAMIC RESPONSE

The FE formulation presented in the preceding section is implemented in a computer program developed by the author using C++. FE analyses evaluate preliminary dynamic response of a poroelastic seabed layer and a poroelastic RMB. Therefore, instabilities resulting from strong ground shaking such as soil liquefaction, excessive soil deformations or bearing capacity failure are not yet modeled in this way. However, even in elastic range there is significant amount of information one can deduce from the analyses. Since there is limited numerical analyses of the response of RMB under seismic waves in the literature (to the best of the author's knowledge), the FE model presented in this study is verified with the one performed by Mase et al. (1994) under surface waves for two types of breakwaters. That is, one including a compacted core relatively stiffer and less permeable than the outer rubble layer while the other being homogeneous and made up of only an outer layer without a core section. Figure 4 illustrates the variation of pore pressure underneath the breakwater for *d*=8m under three wave phases. Results seem to match fairly well except for the region close to the front face where the wave hits the breakwater abruptly which could be due to this transient component.

Following the verification of the numerical model, dynamic response of the system under harmonic seismic waves is obtained for various wave periods and considering two cases for the RMB. These cases are again such that there is a core layer in the middle of the breakwater (Case 1) and the core being absent in the other (Case 2). Dynamic response is computed in terms of pore pressure, effective vertical stress and shear stress distributions along sections 1-1, 2-2 and 3-3 (see Fig. 3) and also horizontally along the still water level (SWL) inside the breakwater. Table 1 summarizes the values of the key parameters used in the analyses. Figures 5-12 present the absolute value of transient response of the variables. It can be seen from the figures that the core layer increases pore pressures rather abruptly, particularly at the seabed-rubble interface while decreasing the effective stress. It

should be noted that the seabed-rubble interface is where the maximum pore pressure is obtained during shaking allowing them to concentrate highly at the toes of the RMB. In the case of nonlinear inelastic response, this may in turn cause numerical instabilities in the subsequent analyses. The stresses and pore water pressure increase in magnitude as the wave period increases. It should again be noted here that this set of results are only preliminary in nature and that they present the weaknesses and strengths of the model and related boundary conditions which still affect the response although artificial damping is applied through Newmark parameters in the time integration scheme.

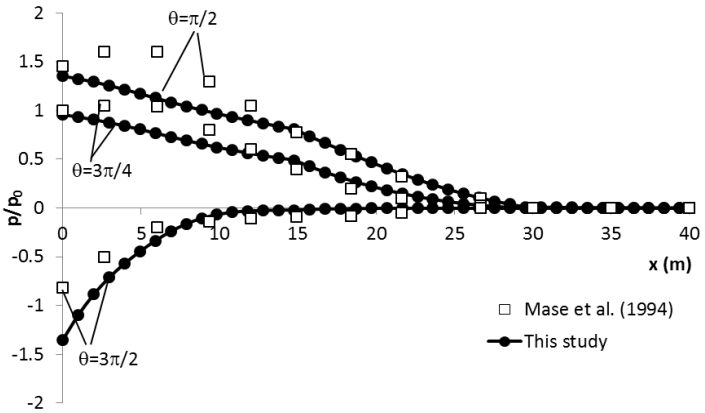

Figure 4. Verification of the numerical model developed in this study with that of Mase et al. (1994) in terms of normalized pore pressure variation with the horizontal

Table 1. Seabed and breakwater properties in FE analyses

Parameter	Seabed	Rubble Mound Outer Layer	Rubble Mound Core
ν	0.33	0.4	0.33
E (MPa)	399	28	266
k_x (m/s)	0.001	0.1	0.01
k_z (m/s)	0.001	0.1	0.01
n	0.28	0.28	0.28
K_f(MPa)	2000	2000	2000
ρ (t/m^3)	1.72	2.0	2.0

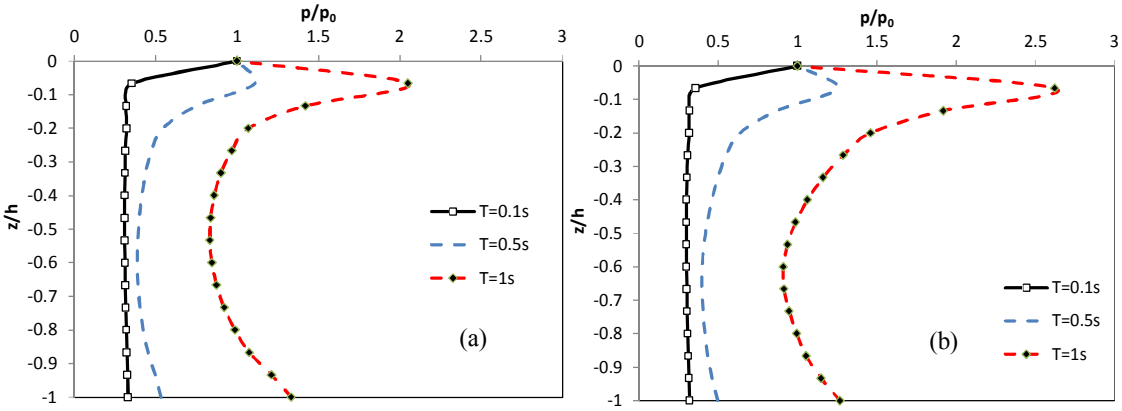

Figure 5. Variation of absolute value of pore pressure at the front toe of rubble, section 1-1, a) Without a core, b) with a core

Figures 13-15 present contour plots of displacements and shear stress for both Case 1 and Case 2 for T=0.5s. It is clear that the core layer in Case 2 decreases horizontal displacement and vertical settlement under seismic wave. This is due to increased stiffness of the breakwater. As far as the shear

stress response, magnitudes in Case 2 are larger due to presence of the core; however, shear stresses are localized in the core and in the transition section from seabed to RMB. The effect of seismic wave period on the dynamic deformations and shear stress is presented in Figure 16 considering Case 2. As the wave period increases, stress and displacement magnitudes grow larger as well. While displacements are mostly taken by the outer layer of rubble mound breakwater which is working as a protective shield, shear stresses concentrate in between the seabed and the rubble mound as well as at the SWL inside the core. It seems the increased normal stresses due to hydrostatic pressure on the breakwater help to develop shearing planes in the core during seismic loading (Figure 16b).

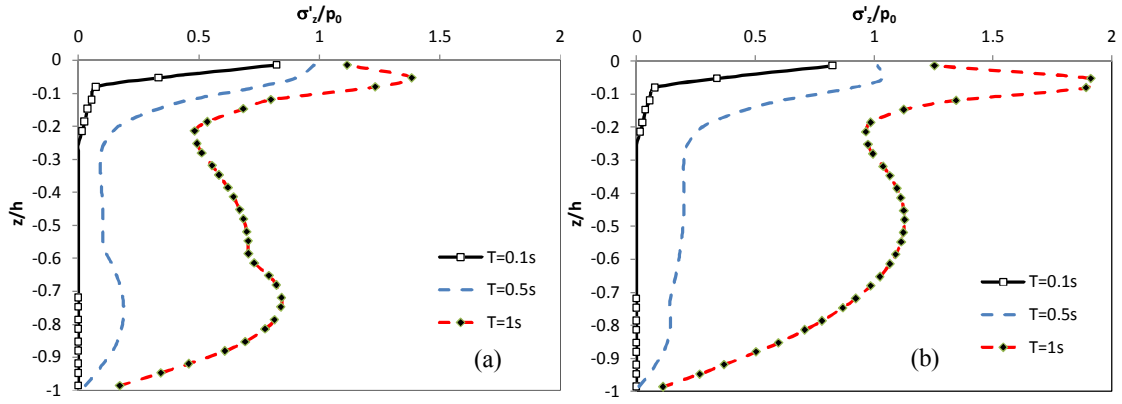

Figure 6. Variation of effective vertical stress at front toe of rubble, section 1-1, a) Without a core, b) with a core

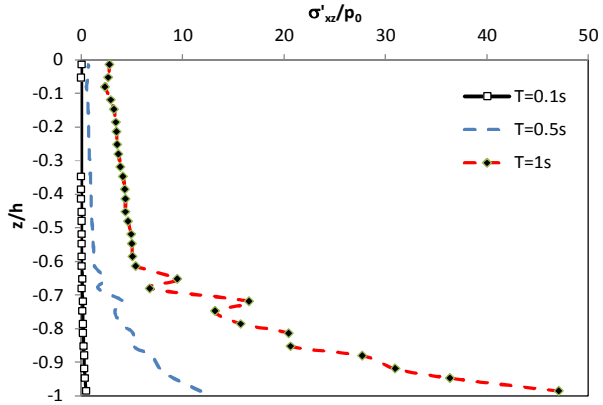

Figure 7. Variation of absolute value of shear stress at the front toe of rubble, section 1-1

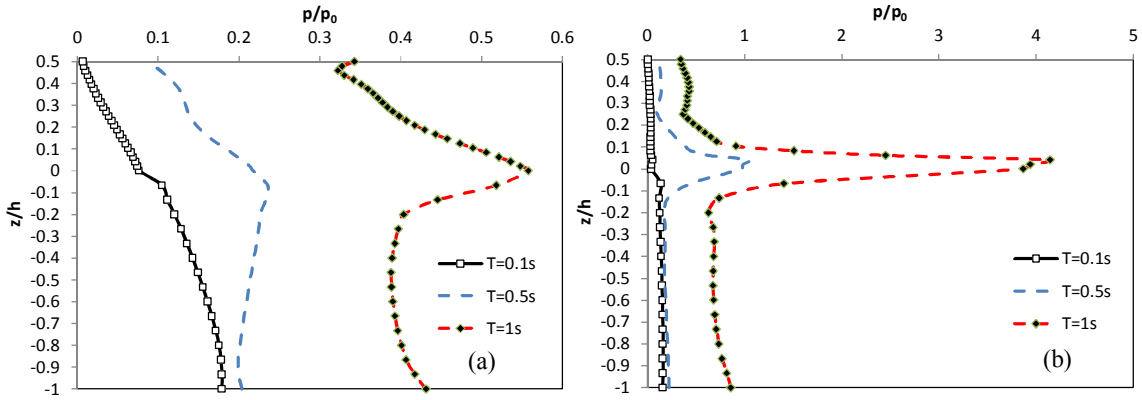

Figure 8. Pore pressure variation at mid-section of seabed-rubble, section 3-3, a) Without a core, b) With a core

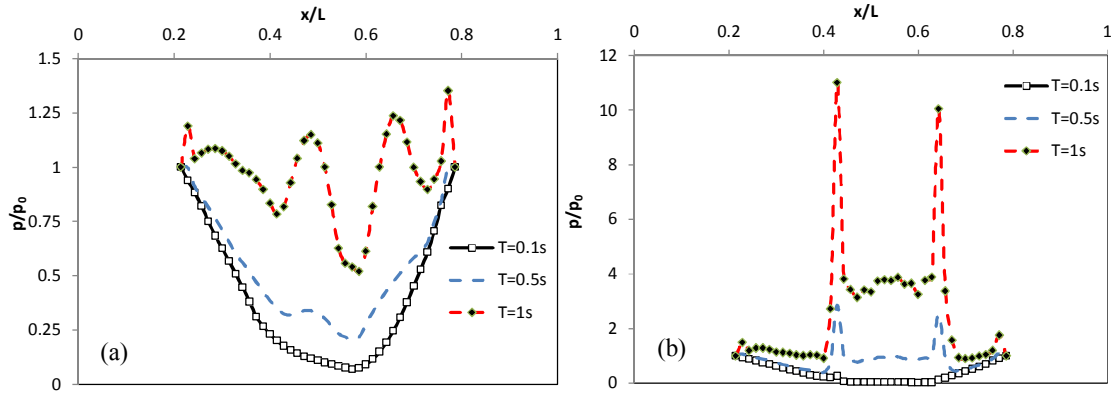

Figure 9. Pore pressure variation at seabed-rubble interface, section 2-2, a) Without a core, b) With a core

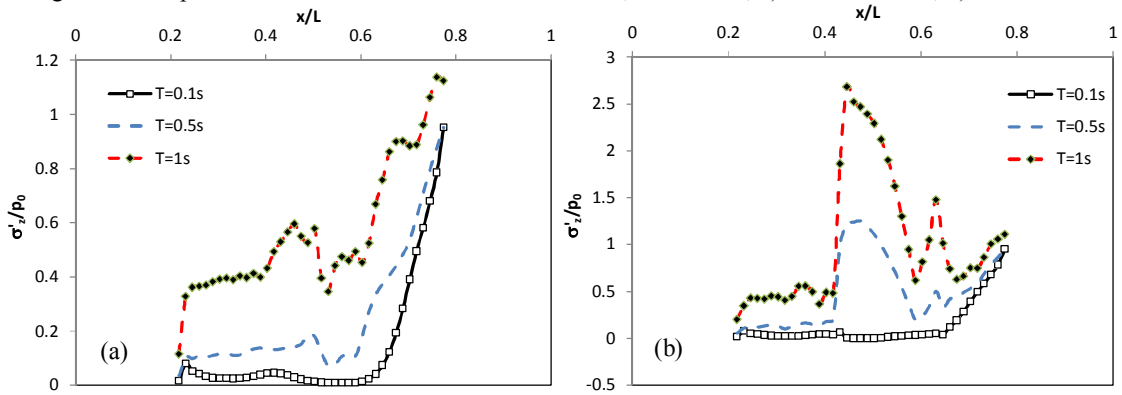

Figure 10. Vertical effective stress at seabed-rubble interface, section 2-2, a) Without a core, b) With a core

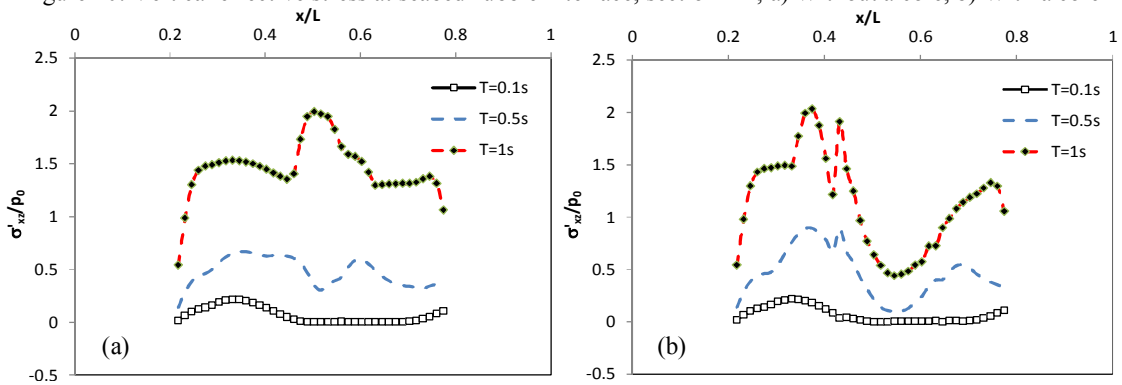

Figure11. Shear stress variation at seabed-rubble interface, section 2-2, a) Without a core, b) With a core

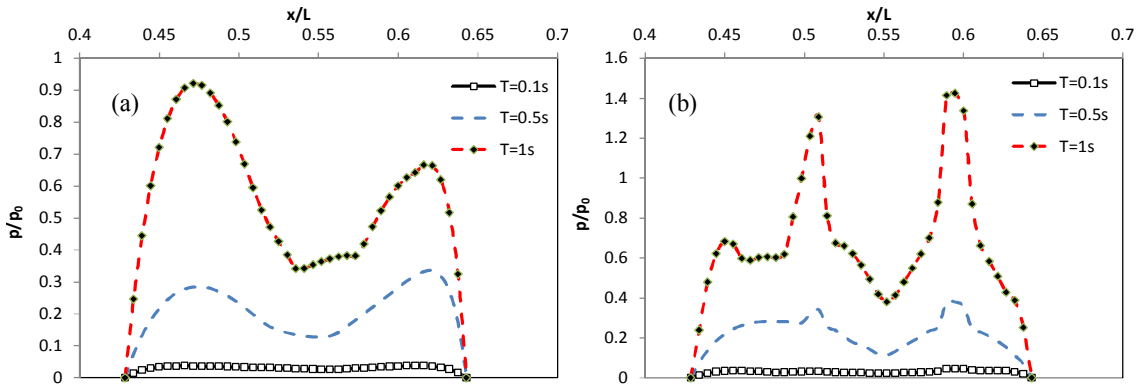

Figure 12. Absolute value of pore pressure at SWL, a) Without a core, b) With a core

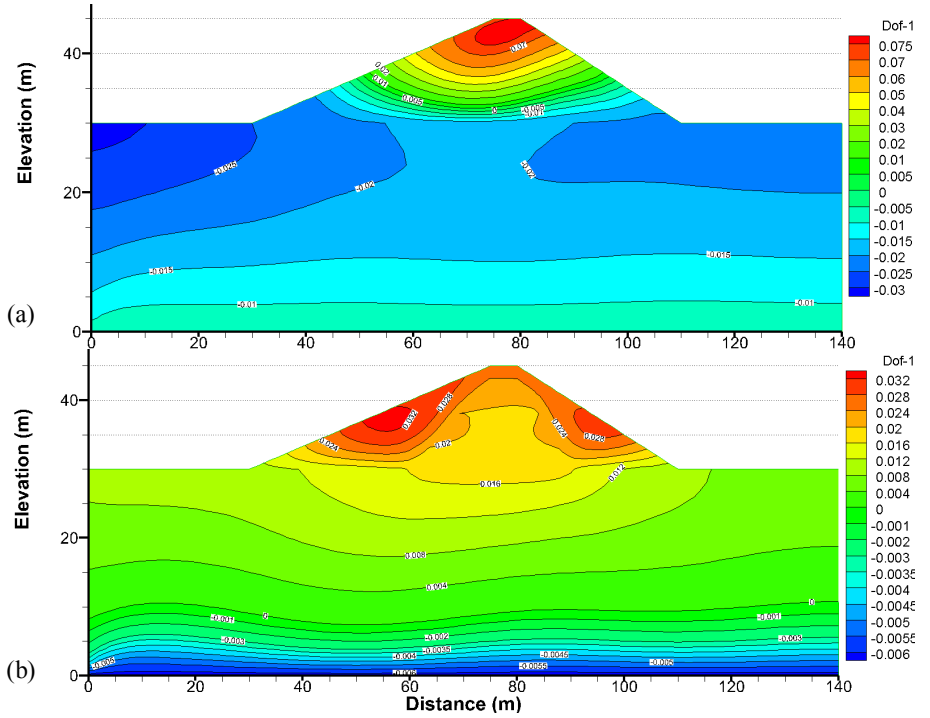

Figure 13. Horizontal displacement (Dof-1 in *m*) contours, a) Without a core, b) With a core

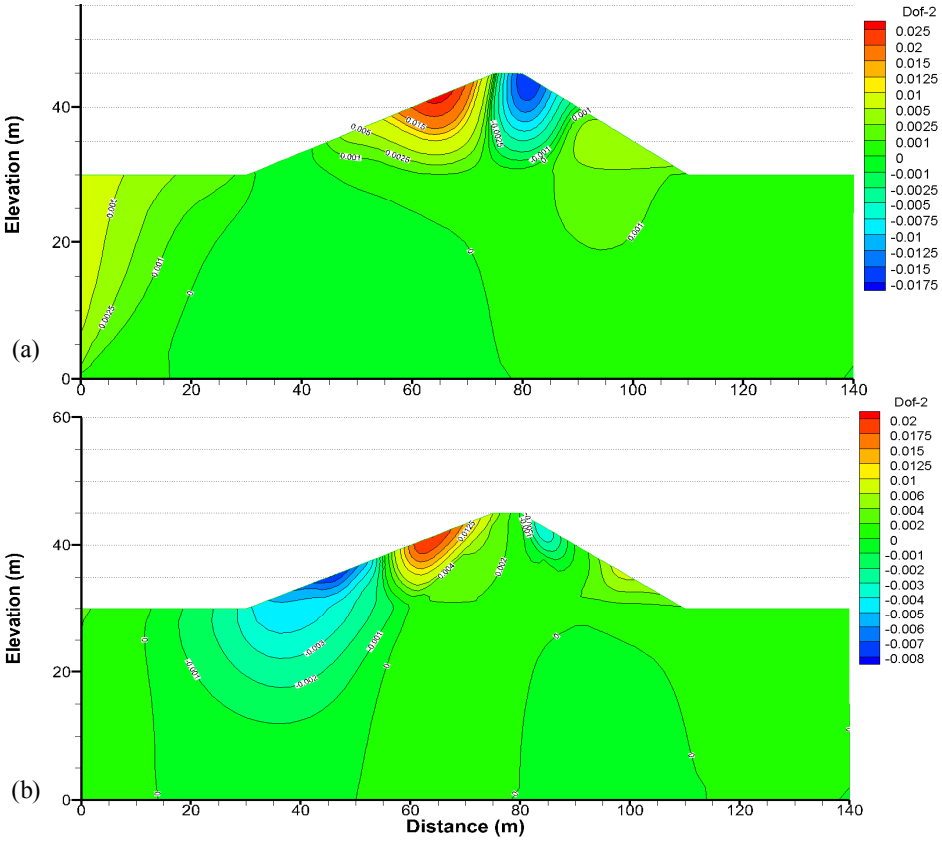

Figure 14. Vertical displacement contours (Dof-2 in *m*), a) Without a core, b) With a core

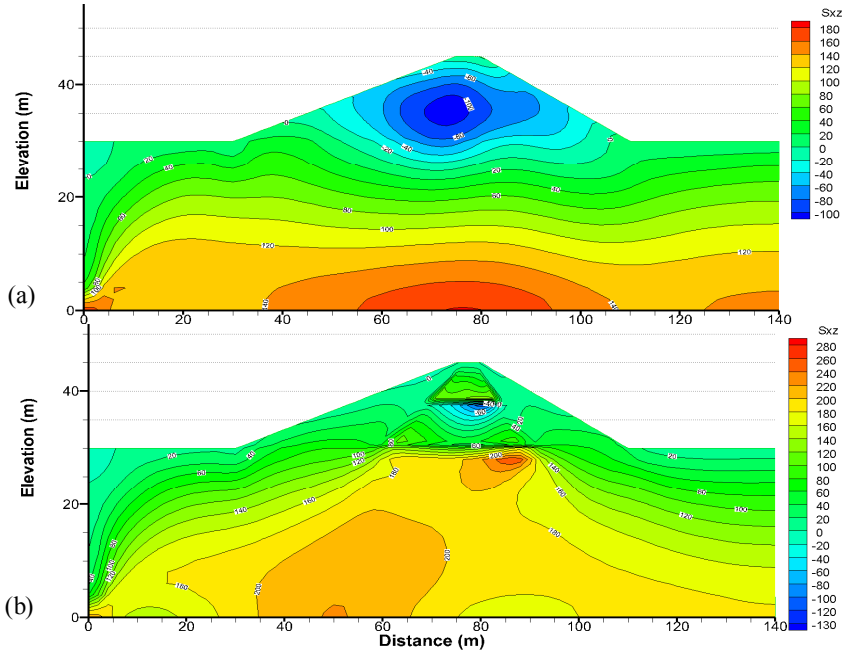

Figure 15. Shear stress contours (Sxz in kPa), a) Without a core, b) With a core

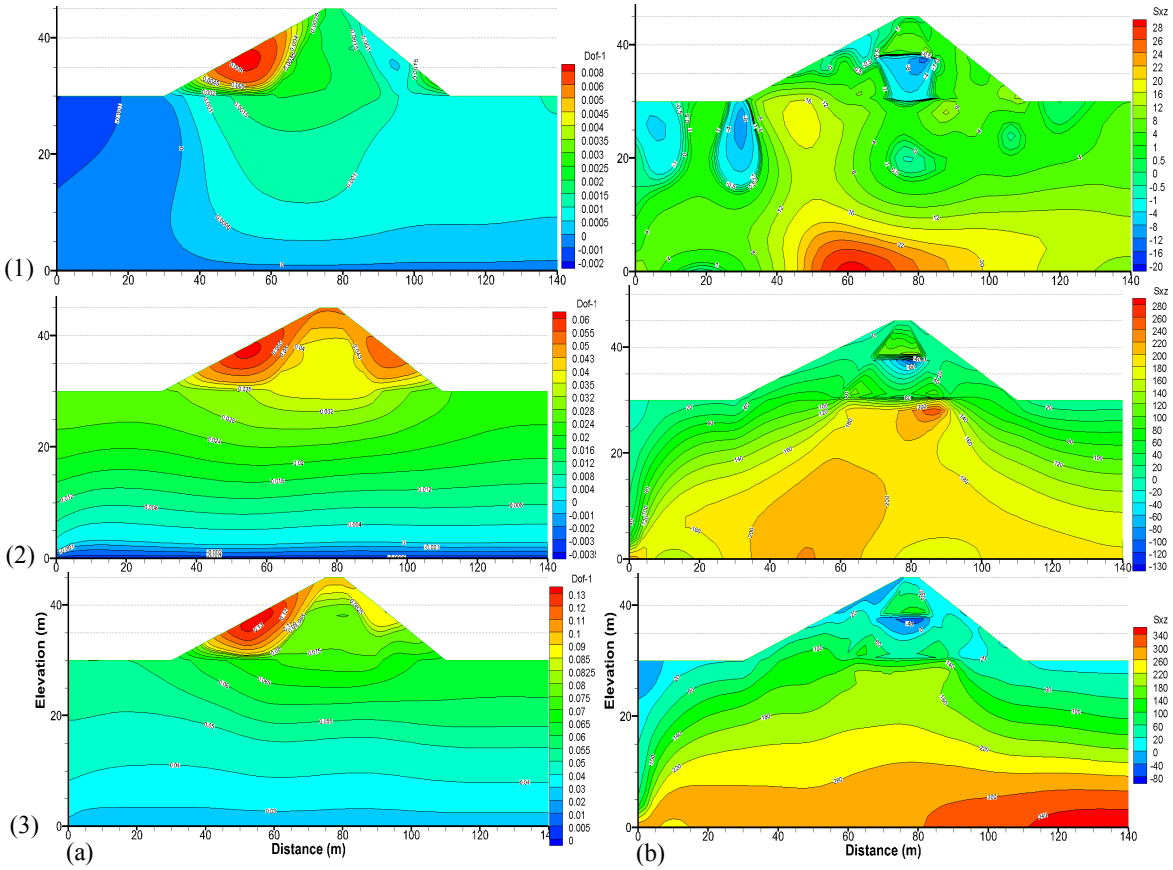

Figure 16. Effect of wave period on a) Horizontal displacement, b) Shear stress variation, 1) T=0.1s, 2) T=0.5s, 3) T=1s in Case 2, values in kPa

CONCLUSIONS

In this study, finite element analysis of a rubble mound breakwater-seabed system under harmonic seismic wave is carried out**.** The seabed and the rubble mound breakwater are assumed to be poroelastic in these preliminary analyses and the dynamic response of the system is assumed to be governed by the poroelasticity equations of coupled flow and deformation. While it is possible to derive three formulations of these equations with respect to inertial terms associated with pore water and soil skeleton, considering the range of frequency of seismic waves, only what is called the *partially dynamic* one is used to capture the dynamic response. Presence of a core decreases displacements and concentrates stresses inside the breakwater requiring further attention through additional and more robust analyses. Overall the core increases the stability during seismic shearing.

REFERENCES

Barends FBJ, Van der Kogel H, Uijttewaal FJ, ad Hagenaal J (1983) "West Breakwater-Sines Dynamic-Geotechnical Stability of Breakwaters", *Proc. of Coastal Structures'83: A Specialty Conf. on Design, Constr., Maint. Performance of Coastal Structures*, Arlington, VA, 31-44.

Biot MA (1941) "General theory of three dimensional consolidation", *J. Applied Physics*, 12:155-164.

Biot MA (1955) "Theory of elasticity and consolidation for a porous anisotropic solid", *Journal of Applied Physics*, 26:182-185.

Biot MA (1962) "Mechanics of deformation and acoustic propagation in porous media", *Journal of Applied Physics*, 33:1482–1498.

De Groot MB, Kudella M, Meijers P, Oumeraci H (2006) "Liquefaction phenomena underneath marine gravity structures subjected to wave loads", *Journal of Waterway, Port, Coastal and Ocean Engineering*, ASCE, 132(4):325-335.

Hur DS, Kim CH, Kim DS and Yoon, JS (2008) "Simulation of the nonlinear dynamic interactions between waves, a submerged breakwater and the seabed", *Ocean Engineering*, 35:511-522.

Jeng DS, Cha DH, Lin YS, Hu PS (2001) "Wave-induced pore pressure around a composite breakwater", *Ocean Engineering*, 28(10):1413-1432.

Losada IJ, Lara JL, Guanche R, Gonzalez Ondima JM (2008) "Numerical analysis of wave-overtopping of rubble-mound breakwaters", *Coastal Engineering*, 55(1):47-62.

Maeno, S. and Nago, H., (1988), "Settlement of a concrete block into a sand bed under wave pressure variation" in Kolkman et al. (Eds.), "Modelling Soil–Water–Structure Interactions", pp. 67-76.

Mase H, Sakai T, Sakamoto M (1994) "Wave-induced pore water pressures and effective stresses around breakwater", *Ocean Engineering*, 21(4):361-379.

Memos C, Bouckovalas G, Tsiachris A (2000) "Stability of rubble mound breakwaters under seismic action", *Coastal Engineering*, 1585-1598, doi: 10.1061/40549(276)123.

Memos CD and Protonotarios, JN (1992) "Patras Breakwater Failure Due to Seismic Loading", *Proc. of the 23rd Int. Conf. on Coastal Engineering*, ASCE, 3343-3356.

Oumeraci H and Partensky, HW (1990) "Wave Induced Pore Pressures in Rubble Mound Breakwaters", *Proc. 22th Int. Conf. on Coastal Engg.*, July 2-6, Delft, Netherlands, 1334-1347.

Palmer GN and Christian, CD (1998) "Design and construction of rubble mound breakwaters", *IPENZ Transactions*, 25(1):19-33.

Rahman MS, El-Zahaby K, Booker JR (1994) "A semi-analytical method for the wave induced seabed response", *Int.J.Anal.Numer.Mthds in Geomech*, 18:213-236.

Ulker MBC, Rahman MS and Guddati, MN (2010) "Wave-induced dynamic response and instability of seabed around a breakwater", *Ocean Engineering*, 37(17-18): 1522-1545.

Ulker MBC, Rahman MS, Guddati, MN (2012) "Breaking wave-induced impact response of rubble mound and seabed around a caisson breakwater", *Int. J. A. Num. Mthd Geo.*, 36(3): 362-390.

Van Gent MRA (1995) "Wave interaction with berm breakwaters", *J. Waterway, Port, Coastal, Ocean Engg*, 121(5):229-238.

Zen K, Umehara Y and Finn, L (1986) "A Case Study of the Wave Induced Liquefaction of Sand Layers under the Damaged Breakwater", *Proc. 3rd Canadian Conf. on Marine Geotechnical Engineering*, St. John's, Newfoundland, 505-520.